Precision Multiboson Phenomenology

G. Bozzi[1], F. Campanario[2, a], C. Englert[3], M. Rauch[2], M. Spannoswky[3], D. Zeppenfeld[2]
[1] *Dipartimento di Fisica, Università di Milano and INFN, Sezione di Milano Via Celoria 16, I-20133 Milano, Italy*
[2] *Institute für Theoretische Physik, Universität Karlsruhe, KIT, 76128 Karlsruhe, Germany*
[3] *Institut for Particle Physics Phenomenology, Department of Physics, Durham University, Durham, United Kingdom*

We present recent results in precision multiboson (+jet) phenomenology at the LHC. Results for diboson + jet, triboson, and also for $W^{\pm}\gamma\gamma+$ jet will be discussed focusing on the impact of the perturbative corrections on the expected phenomenology.

1 Introduction

Processes with multiple electroweak bosons are important channels to test the Standard Model (SM) at the LHC. They are important backgrounds to SM and also to beyond standard physics searches. As a signal, they allow us to obtain information on triple and quartic couplings, and therefore, to quantify deviations from the SM prediction through, e.g., anomalous couplings.

To match the experimental accuracy, precise and reliable predictions beyond the leading order (LO) perturbative expansion are required not only for cross sections but also for differential distributions. As part of such a program we have, in the past, determined next-to-leading-order (NLO) QCD corrections for the production cross sections of all combinations of three electroweak bosons [1,2], to $W\gamma$ + jet [3,4] , WZ + jet [5,6] and also to $W^{\pm}\gamma\gamma+$ jet [7], available in the VBFNLO package [8]. In all cases, leptonic decays of the electroweak bosons were included in the calculations. For the production of three weak bosons and also for $W^{\pm}\gamma\gamma$, these results were verified against independent calculations [9,10,11] which are available for on-shell bosons and neglecting Higgs boson exchange.

In these proceedings, we review results for $W^{\pm}\gamma\gamma$, $W^{\pm}\gamma\gamma$ + jet and $W^{\pm}\gamma/W^{\pm}Z$ +jet, including their leptonic decays and full off-shell effects, in Section 2, 3 and 4, respectively, for the LHC at 14 TeV. We summarize in Section 5.

2 $W^{\pm}\gamma\gamma$

Among the triple vector boson production channels, $W^{\pm}\gamma\gamma$ has turned out to be of particular interest. $W^{\pm}\gamma\gamma$ production is sensitive to the $WW\gamma$ and $WW\gamma\gamma$ vertices [12]. In addition, a final state with two photons and missing transverse energy is relevant in a variety of beyond

[a] Speaker, based on a talk given at the 47th Rencontres de Moriond on QCD and High Energy Interactions, March 10-17, 2012, La Thuile, Italy.

the standard model scenarios [13]: in gauge-mediated supersymmetry breaking, for instance, the neutralino is often the next-to-lightest supersymmetric particle and decays into a photon plus a gravitino, giving a signal of two photons and missing E_T. In Ref. [14], a study of the backgrounds for supersymmetry motivated di-photon production searches has been performed, pointing out the relevance of the $W^{\pm}\gamma\gamma$ production process as a SM background in case of electron misidentification. Another possible application is an estimate of backgrounds when searching for WH production, followed by Higgs decay to two photons.

We compute the NLO hadronic cross section by straightforward application of the Catani-Seymour dipole subtraction [15]. The loop contributions are evaluated using the Passarino-Veltman scheme up to four-point functions [16] and the Denner-Dittmaier reduction [17] for five point integrals and we perform various cross checks to validate our implementation, Refs. [2,18].

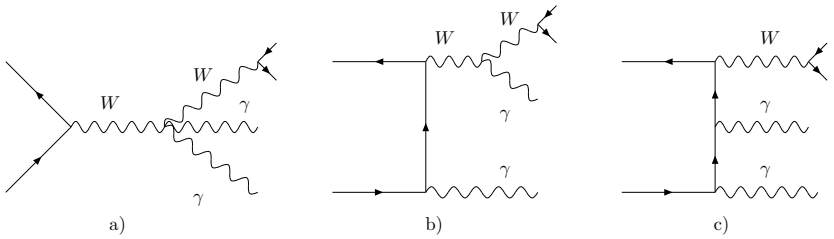

Figure 1: Example of the three topologies contributing to $pp \to l\nu\gamma\gamma$ + X

The NLO virtual corrections result from one-loop diagrams obtained by attaching a gluon line to the quark-antiquark line in diagrams like the ones depicted in Fig. 1. We combine the virtual corrections into three different groups, which include all loop diagrams derived from a given Born level configuration. This leaves us with three universal building blocks, namely factorizable corrections (Virtual-born) and corrections to two (Virtual-box) or three (Virtual-Pentagons) vector bosons attached to the quark line. For our numerical results, we use the CT10 parton distribution set [19] with $\alpha_s(m_Z) = 0.118$ at NLO, and the CTEQ6L1 set [20] with $\alpha_s(m_Z) = 0.130$ at LO. We impose a set of minimal cuts on leptons, photons and jets, namely,

$$p_{T\ell(\gamma)} > 20 \text{ GeV} \qquad |y_{\ell(\gamma)}| < 2.5 \qquad R_{\gamma\gamma} > 0.4 \qquad R_{\ell\gamma} > 0.4 \qquad R_{j\ell} > 0.4 \qquad R_{j\gamma} > 0.7 \quad (1)$$

as well as an isolation criteria à la Frixione [21] for the photons,

$$\Sigma_i \, E_{T_i} \, \theta(\delta - R_{i\gamma}) \, \leq \, p_{T\gamma} \, \frac{1-\cos\delta}{1-\cos\delta_0} \qquad (\text{for all} \quad \delta \leq \delta_0), \tag{2}$$

where δ_0 is a fixed separation which is set to 0.7. We consider $W^{\pm}$ decays to the first two lepton generations, i.e., $W \to e\nu_e(+\gamma), \mu\nu_\mu(+\gamma)$ and these contributions have been summed in Fig. 2, where we show numerical results for $W^+\gamma\gamma$ production within the cuts of Eqs. (1, 2). On the left panel, we show the overall scale variation of our numerical predictions at LO and NLO: the NLO K-factor is large both in absolute value (~ 3) and compared to the LO scale variation. The NLO scale uncertainty is about 10% when varying the factorization and the renormalization scale $\mu = \mu_F = \mu_R$ up and down by a factor 2 around the reference scale $\mu_0 = m_{W\gamma\gamma}$ and is mainly driven by the dependence on μ_R. The large size of the NLO corrections partially originates from new gluon induced channels entering first at NLO, $gq \to W^{\pm}\gamma\gamma\, q$, which are α_s suppressed, but enhanced by the large gluon pdfs at the LHC. Since these 1-jet contributions to the $\mathcal{O}(\alpha_s)$ cross section are only determined at LO, and are unbalanced against the virtual part, their scale variation is large. In fact, most of the scale variation of the total NLO result is accounted for by the real emission contributions, defined here as the real emission cross section

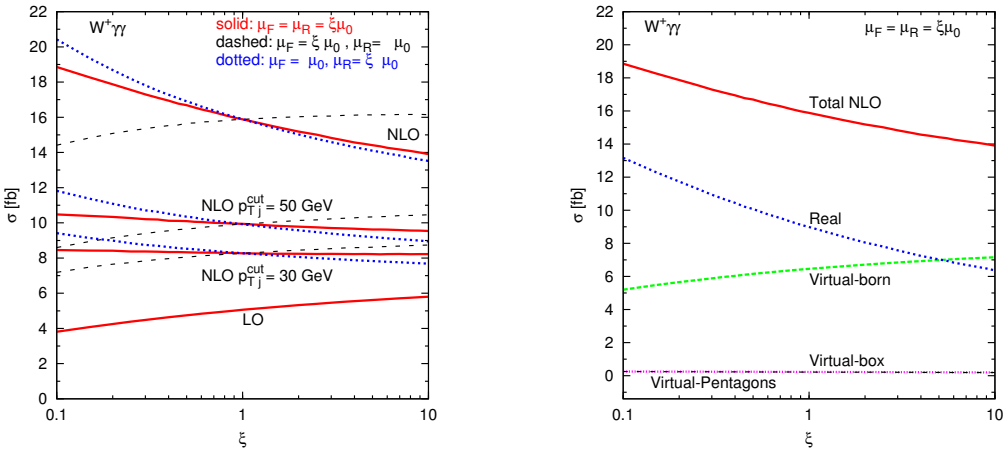

Figure 2: *Left:* Scale dependence of the total LHC cross section for $pp \to \ell^+\gamma\gamma + \not{p}_T + X$ at at LO and NLO, within the cuts of Eqs. (1,2). The factorization and renormalization scales are varied in the range from $0.1 \cdot \mu_0$ to $10 \cdot \mu_0$. *Right:* Same as in the left panel but for the different NLO contributions at $\mu_F = \mu_R = \xi\mu_0$.

minus the Catani-Seymour subtraction terms plus the finite collinear terms. This is more visible in the right panels, where we show the scale dependence and compare the size of the different parts of the NLO calculation. As for the relative size of the NLO terms, the real emission contributions dominate and are even larger than the LO terms plus virtual terms proportional to the Born amplitude. Non-trivial virtual contributions, namely the interference of the Born amplitude with virtual-box and virtual-pentagon contributions, represent less than 1% of the total result and their scale dependence is basically flat. In the left panels, we also show results for additional jet veto cuts, requiring $p_{Tj} < 50$ GeV or $p_{Tj} < 30$ GeV. While it is evident that the renormalization scale variation is highly reduced by a jet veto, this reduction should not be interpreted as a smaller uncertainty of the vetoed cross section: a similar effect in $W^\pm\gamma j$ and WZj and $W^\pm\gamma\gamma j$ production could be traced to cancellations between different regions of phase space and, thus, the small variation is cut-dependent [5] as shown in the following sections.

Among the triple vector boson production channels, $W^\pm\gamma\gamma$ production is the one with the largest K-factor for the integrated cross section. In Ref.[2] (see also [11]), it was shown that this is due to cancellations at LO driven by a radiation zero [22]. The radiation zero at NLO is obscured, similar to $W^\pm\gamma$ production [25], by additional real QCD radiation, $W^\pm\gamma\gamma$ +jet, as part of the NLO contributions. An additional jet veto-cut might help in the detection of the radiation zero, while reducing also the scale uncertainties for the relevant distributions. However, this procedure raises the question of the reliability of the predictions due to the aforementioned problem with the exclusive vetoed samples. Furthermore, the remaining scale uncertainties at NLO QCD are due to unbalanced gluon-induced real radiation computed at LO, e.g., $gq \to W^\pm\gamma\gamma\ q$. To realistically asses the uncertainties, also concerning anomalous coupling searches, and as an important step towards a NNLO QCD calculation of $W^\pm\gamma\gamma$, we have calculated $W^\pm\gamma\gamma$ +jet at NLO QCD.

3 $W^\pm\gamma\gamma$+ jet

This is the first calculation falling in the category of $VVV + j$, which includes the evaluation of the complex hexagon virtual amplitudes, which poses a challenge not only at the level of the analytical calculation, but also concerning the CPU time required to perform a full $2 \to 4$ process at NLO QCD.

For the virtual contributions we use the routines computed in Ref. [18]. At the numerical

evaluation level, we split the virtual contributions into fermionic loops (Virtual-fermionbox) and bosonic contributions with one (Virtual-box), two (Virtual-pentagons) and three (Virtual-hexagons) electroweak vector bosons attached to the quark line. This procedure allows us to drastically reduce the time spent in evaluating the part containing hexagon diagrams as explained in Refs. [7,18]. The numerical stability of the hexagons' contributions is discussed in detail in Ref. [18].

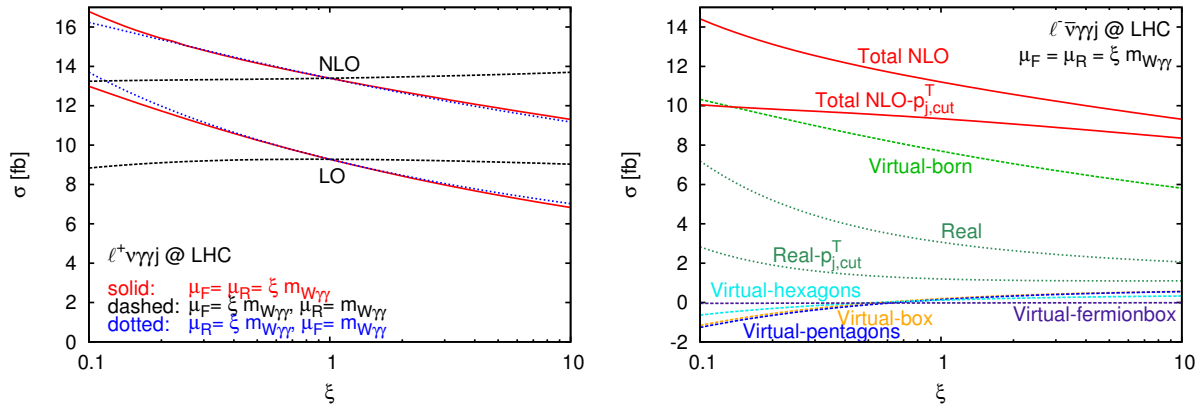

Figure 3: Scale variation of the $\ell^\pm\nu\gamma\gamma$+jet production cross sections at the LHC ($\ell = e, \mu$). The cuts are described in the text and we choose $\mu_R = \mu_F = m_{W\gamma\gamma}$ as central dynamical reference scale. The right panel shows the individual contributions to the NLO cross section according to our classification of topologies. We also show results where we have applied a veto on events with two identified jets having both $p_T^j > 50$ GeV

We use the same input parameters as for $W^\pm\gamma\gamma$ production and apply the cuts of Eqs. (1,2). Further details on the parameter choices can be found in Ref. [7]. Again, we consider $W^\pm$ decays to the first two lepton generations, i.e, $W \to e\nu_e(+\gamma), \mu\nu_\mu(+\gamma)$ and these contributions have been summed in Fig 3 and 4.

We compute total K factors of 1.43 (1.48) for $W^+\gamma\gamma$+jet ($W^-\gamma\gamma$+jet) production at the LHC, values which are quite typical for multiboson+jet production as found in Refs. [4,6,24] and partially originated by new e.g, gg and qq induced channels. This moderate K-factor (as compared to corrections of $\sim 300\%$ for $W^\pm\gamma\gamma$ production) indicates, as expected, that the $W^\pm\gamma\gamma$ + jet production channel is not affected by radiation zero cancellations.

The scale dependences of the $W^+\gamma\gamma j$ and $W^-\gamma\gamma j$ production cross sections turn out to be modest: when comparing $\mu_R = \mu_F = \xi m_{W\gamma\gamma}$ for $\xi = 0.5$ and $\xi = 2$, we find differences of 10.8% (12.0%), respectively, see Fig. 3.

The phase space dependence of the QCD corrections is non-trivial and sizable (we again choose $\mu_R = \mu_F = m_{W\gamma\gamma}$). Vetoed real-emission distributions are plagued with large uncertainties (Fig.4, left) — a characteristic trait well-known from VV+jet phenomenology [5,24]. Additional parton emission modifies the transverse momentum and invariant mass spectra in particular. The leading jet becomes slightly harder at NLO as can be inferred from the differential K factor in the bottom panel of Fig. 4. When comparing precisely measured distributions in this channel against LO Monte Carlo predictions, the not-included QCD corrections could be misinterpreted for anomalous electroweak trilinear or quartic couplings [4,6,25] arising from new interactions beyond the SM.

4 $W^\pm\gamma/W^\pm Z$ + jet

NLO corrections to $pp \to W^\pm\gamma/W^\pm Z$ +jet cross section have been computed in Refs. [3,5], and including anomalous couplings in Refs. [4,6]. All off-shell effects were included. Similar observations as in $W^\pm\gamma\gamma$ + jet were found. When varying the factorization and renormalization scale by a

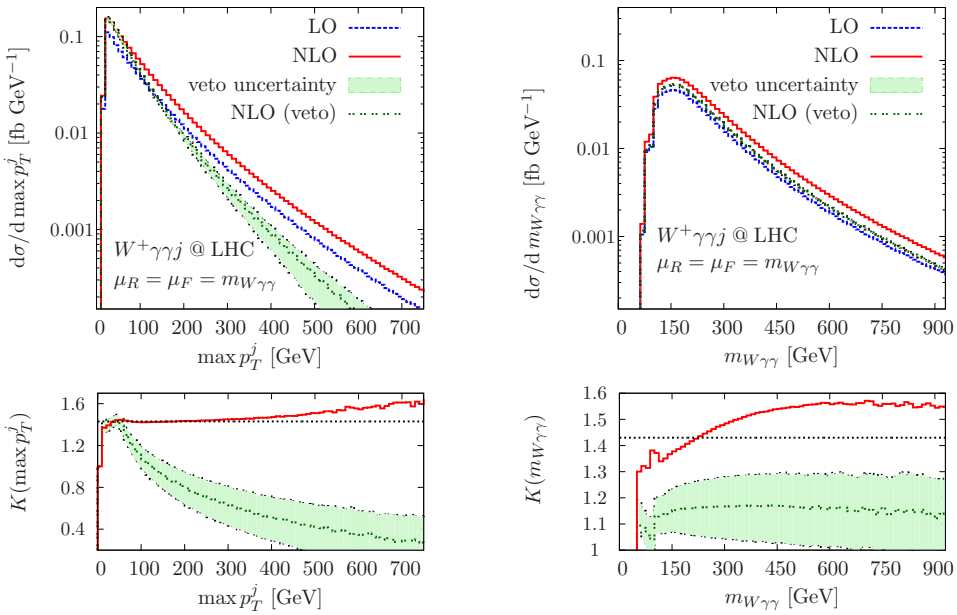

Figure 4: Differential $\max p_T^j$ and $m_{W\gamma\gamma}$ distribution for inclusive and exclusive $l^+\bar{\nu}\gamma\gamma$+jet production.

factor 2 around fixed values of μ_0=100 GeV, one finds modest scale variations. Vetoed samples pick up large uncertainties (Fig.5, left). K-factors are around 1.4 at the LHC and they vary over phase space. Two examples are shown for these processes in Fig. 5, including the sensitivity to anomalous couplings in the p_T^γ differential distributions for $W^\pm\gamma$ +jet production for different choices of anomalous parameters (λ_0, k_0).

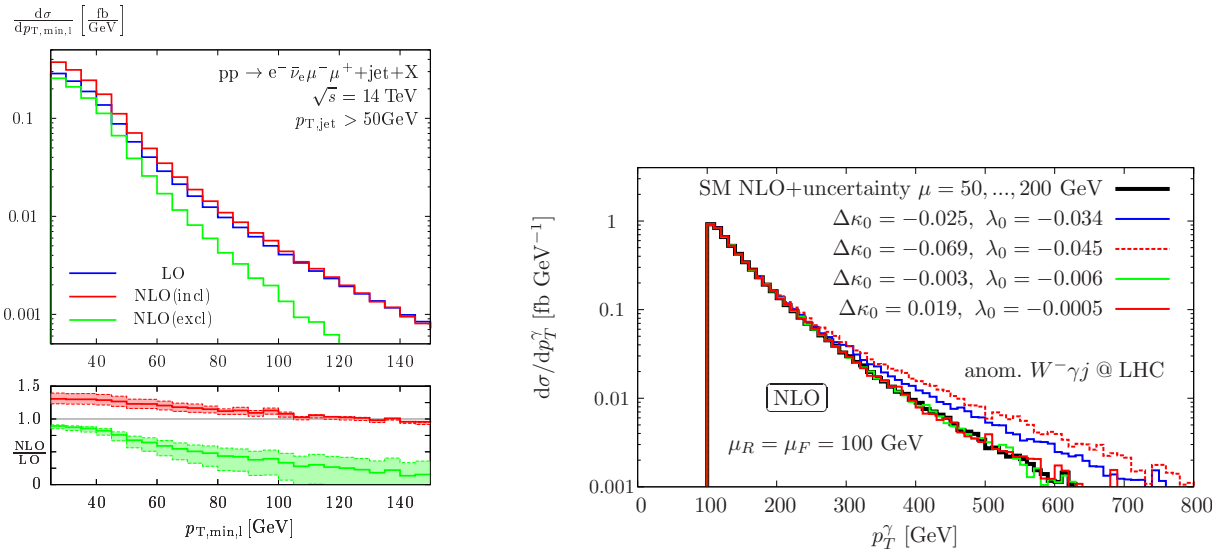

Figure 5: *Left:* Differential distribution for $p_{T,min,l}$ for inclusive and exclusive W^-Z+jet production. *Right:* Sensitivity to anomalous couplings for $l^-\nu\gamma$ + jet in the p_T^γ distribution.

5 Summary

The QCD corrections for vector boson production in the diboson + jet, triboson and triboson + jet channels are large and exceed the expectations driven by LO scale uncertainties. Total K-

factors up to 3 for $W^{\pm}\gamma\gamma$ have been reported. The size of the QCD corrections for $W^{\pm}\gamma/W^{\pm}Z$ + jet and $W^{\pm}\gamma\gamma$ + jet production is around the 40% level. Corrections can be larger for differential distributions and therefore have to be considered for a precise comparison of data to SM predictions for all these processes. Finally, we have shown that the diboson + jet production channels are sensitive to anomalous coupling searches through differential distributions.

References

1. V. Hankele and D. Zeppenfeld, Phys. Lett. B **661** (2008) 103; F. Campanario, V. Hankele, C. Oleari, S. Prestel and D. Zeppenfeld, Phys. Rev. D **78** (2008) 094012; G. Bozzi, F. Campanario, V. Hankele and D. Zeppenfeld, Phys. Rev. D **81** (2010) 094030; G. Bozzi, F. Campanario, M. Rauch, H. Rzehak and D. Zeppenfeld, Phys. Lett. B **696**, 4 (2011); G. Bozzi, F. Campanario, M. Rauch and D. Zeppenfeld, Phys. Rev. D **84** (2011) 074028.
2. G. Bozzi, F. Campanario, M. Rauch and D. Zeppenfeld, Phys. Rev. D **83** (2011) 114035.
3. F. Campanario, C. Englert, M. Spannowsky and D. Zeppenfeld, Europhys. Lett. **88** (2009) 11001.
4. F. Campanario, C. Englert and M. Spannowsky, Phys. Rev. D **83** (2011) 074009.
5. F. Campanario, C. Englert, S. Kallweit, M. Spannowsky and D. Zeppenfeld, JHEP **1007** (2010) 076.
6. F. Campanario, C. Englert and M. Spannowsky, Phys. Rev. D **82** (2010) 054015.
7. F. Campanario, C. Englert, M. Rauch and D. Zeppenfeld, Phys. Lett. B **704** (2011) 515.
8. K. Arnold *et al.*, Comput. Phys. Commun. **180** (2009) 1661; arXiv:1107.4038 [hep-ph].
9. A. Lazopoulos, K. Melnikov and F. Petriello, Phys. Rev. D **76** (2007) 014001.
10. T. Binoth, G. Ossola, C. G. Papadopoulos and R. Pittau, JHEP **0806** (2008) 082.
11. U. Baur, D. Wackeroth and M. M. Weber, PoS **RADCOR2009**, 067 (2010) [arXiv:1001.2688 [hep-ph]]; M. M .Weber, private communication.
12. S. Godfrey, arXiv:hep-ph/9505252; P. J. Dervan, A. Signer, W. J. Stirling and A. Werthenbach, J. Phys. G **26** (2000) 607; O. J. P. Eboli, M. C. Gonzalez-Garcia, S. M. Lietti and S. F. Novaes, Phys. Rev. D **63** (2001) 075008; P. J. Bell, arXiv:0907.5299 [hep-ph]; M. Dobbs, AIP Conf. Proc. **753** (2005) 181-192.
13. J. M. Campbell, J. W. Huston and W. J. Stirling, Rept. Prog. Phys. **70**, 89 (2007).
14. CMS Collaboration, CMS-PAS-SUS-09-004, (2009).
15. S. Catani and M. H. Seymour, Nucl. Phys. B **485** (1997) 291 [Erratum-ibid. B **510** (1998) 503].
16. G. Passarino and M. J. G. Veltman, Nucl. Phys. B **160**, 151 (1979).
17. A. Denner and S. Dittmaier, Nucl. Phys. B **658**, 175 (2003); Nucl. Phys. B **734**, 62 (2006).
18. F. Campanario, JHEP **1110** (2011) 070.
19. H. -L. Lai, M. Guzzi, J. Huston *et al.*, Phys. Rev. **D82** (2010) 074024.
20. J. Pumplin, D. R. Stump, J. Huston, H. L. Lai, P. Nadolsky and W. K. Tung, JHEP **0207** (2002) 012.
21. S. Frixione, Phys. Lett. B **429**, 369 (1998).
22. R. W. Brown, K. L. Kowalski, S. J. Brodsky, Phys. Rev. **D28** (1983) 624.
23. U. Baur, T. Han, J. Ohnemus, Phys. Rev. **D48** (1993) 5140-5161.
24. V. Del Duca, F. Maltoni, Z. Nagy and Z. Trocsanyi, JHEP **0304** (2003) 059. S. Dittmaier, S. Kallweit and P. Uwer, Phys. Rev. Lett. **100**, 062003 (2008); Nucl. Phys. B **826** (2010) 18. T. Binoth, T. Gleisberg, S. Karg, N. Kauer and G. Sanguinetti, Phys. Lett. B **683**, 154 (2010).
25. U. Baur, T. Han and J. Ohnemus, Phys. Rev. D **48** (1993) 5140. J. M. Campbell, R. K. Ellis and C. Williams, JHEP **1107**, 018 (2011).